An Isothermal Titration Calorimetry Study of the Binding of Substrates and Ligands to the Tartrate Dehydrogenase from *Pseudomonas putida* Reveals Half-of-the-Sites Reactivity†

William E. Karsten and Paul F. Cook*

Department of Chemistry and Biochemistry, University of Oklahoma, 620 Parrington Oval, Norman, Oklahoma 73019

Received April 14, 2006; Revised Manuscript Received May 25, 2006

ABSTRACT: An isothermal titration calorimetric study of the binding of substrates and inhibitors to different complexes of tartrate dehydrogenase (TDH) from *Pseudomonas putida* was carried out. TDH catalyzes the nicotinamide adenine dinucleotide (NAD)-dependent oxidative decarboxylation of D-malate and has an absolute requirement for both a divalent and monovalent metal ion for activity. The ligands Mn^{2+}, *meso*-tartrate, oxalate, and reduced nicotinamide adenine dinucleotide (NADH) bound to all TDH complexes with a stoichiometry of 1 per enzyme dimer. The exception is NAD, which binds to E/K^+, $E/K^+/Mn^{2+}$, and $E/K^+/Mg^{2+}$ complexes with a stoichiometry of two per enzyme dimer. The binding studies suggest a half-of-the-sites mechanism for TDH. No significant heat changes were observed for D-malate in the presence of the $E/K^+/Mn^{2+}$ complex, suggesting that it did not bind. In contrast, *meso*-tartrate does bind to $E/K^+/Mn^{2+}$ but gives no significant heat change in the presence of E/Mn^{2+}, suggesting that K^+ is required for *meso*-tartrate binding. *meso*-Tartrate also binds with a large ΔC_p value and likely binds via a different binding mode than D-malate, which binds only in the presence of NAD. In contrast to all of the other ligands tested, the binding of Mn^{2+} is entropically driven, likely the result of the entropically favored disruption of ordered water molecules coordinated to Mn^{2+} in solution that are lost upon binding to the enzyme. Oxalate, a competitive inhibitor of malate, binds with the greatest affinity to $E/K^+/Mn^{2+}$/NADH, and its binding is associated with the uptake of a proton. Overall, with D-malate as the substrate, data are consistent with a random addition of K^+, Mn^{2+}, and NAD followed by the ordered addition of D-malate; there is significant synergism in the binding of NAD and K^+. Although the binding of *meso*-tartrate also requires enzyme-bound K^+ and Mn^{2+}, the binding of *meso*-tartrate and NAD is random.

The tartrate dehydrogenase (TDH)[1] from *Pseudomonas putida* is a homodimer with a subunit M_r of 40 636 (*1*, *2*). The enzyme is reported to catalyze three distinct nicotinamide adenine dinucleotide (NAD)-dependent reactions, the oxidative decarboxylation of D-malate to pyruvate and CO_2, the oxidation of (+)-tartrate to oxaloglycolate, and the formation of D-glycerate and CO_2 from *meso*-tartrate (*1*). The *meso*-tartrate reaction is thought to occur with no net production of reduced nicotinamide adenine dinucleotide (NADH); the enolate of hydroxypyruvate produced during the reaction is believed to remain on the enzyme and be reduced by the bound NADH, which was produced in the initial oxidation of *meso*-tartrate. The enzyme shows the greatest activity in the oxidative decarboxylation of D-malate ($V/E_t = 9\ s^{-1}$) compared to the oxidation of (+)-tartrate ($V/E_t = 0.6\ s^{-1}$) (*3*).

The enzyme requires both a monovalent and divalent metal ion for activity. The best monovalent metal ion for activity is K^+. Both Mg^{2+} and Mn^{2+} support catalysis; however, on the basis of initial velocity studies, Mn^{2+} binds to the enzyme with about a 40-fold greater affinity than Mg^{2+}. The kinetic mechanism of TDH with either D-malate or (+)-tartrate as the substrate is reported to be ordered with the divalent metal ion binding first followed by NAD and either D-malate or (+)-tartrate (*1*). On the basis of multiple-isotope-effect studies, the oxidative decarboxylation reaction with D-malate is stepwise (*3*). The initial step is oxidation of D-malate to form an oxaloacetate intermediate, which then decarboxylates with a Lewis acid assistance from the divalent metal ion to give enolpyruvate. The enolpyruvate intermediate is tautomerized to the final product pyruvate with assistance from an enzymatic general acid. It has been proposed that oxalate is an analogue of the enolpyruvate intermediate formed during the TDH reaction and is a slow-binding inhibitor of the TDH reaction (*4*).

To further investigate the TDH reaction, an isothermal titration calorimetric study of the binding of substrates and inhibitors was carried out to determine the binding constants and thermodynamic parameters associated with binding. In addition, the kinetic mechanism of TDH was re-examined in light of the isothermal titration calorimetry (ITC) results

† This work was supported by a grant to P.F.C. from the National Science Foundation (MCB 0091207) and the Grayce B. Kerr endowment to the University of Oklahoma to support the research of P.F.C.

* To whom correspondence should be addressed. Telephone: 405-325-4581. Fax: 405-325-7182. E-mail: pcook@ou.edu.

[1] Abbreviations: IPMDH, isopropylmalate dehydrogenase; Hepes, *N*-(2-hydroxyethyl)piperazine-*N*′-2-ethanesulfonic acid; ITC, isothermal titration calorimetry; NAD, nicotinamide adenine dinucleotide (the + sign is omitted for convenience): NADH, reduced nicotinamide adenine dinucleotide; TDH, tartrate dehydrogenase; Tris, tris(hydroxymethyl)-aminomethane.

10.1021/bi0607251 CCC: $33.50
Published on Web 06/29/2006

and also to investigate the role of the K^+ ion in the kinetic mechanism.

MATERIALS AND METHODS

Chemicals. The chemicals were acquired from the following companies: $MgSO_4$, $MnSO_4$, and oxalate from Fisher; D-malate, (+)-tartrate, and *meso*-tartrate from Sigma; NAD and NADH from Sigma or USB; and *N*-(2-hydroxyethyl)piperazine-*N*′-2-ethanesulfonic acid (Hepes) and tris(hydroxymethyl)aminomethane (Tris) from Research Organics. All chemicals were used without further purification. The enzyme was isolated from *Escherichia coli* cells harboring the plasmid pTDH1 (*2*) and purified according to a previously published method (*3*). The enzyme was >95% pure on the basis of sodium dodecyl sulfate−polyacrylamide gel electrophoresie (SDS−PAGE).

ITC. Titrations were carried out with a Micro Calorimetry System from MicroCal, Inc. The stirred cell contained TDH at a typical concentration of about 0.2 mM (enzyme monomer). Protein concentrations were determined either by the method of Bradford (*5*) using bovine serum albumin as a standard or by the intrinsic enzyme absorbance at 280 nm (ϵ = 61 360 M^{-1} cm^{-1}) (6). The protein concentrations determined by the two methods were identical within error. In addition to the enzyme, the stirred cell typically contained one or more of the metal ion cofactors (Mn^{2+} or K^+) and substrates at a concentration greater than 10 times their respective K_d. The injection syringe contained substrates or inhibitors at a concentration of 2−10 mM depending upon the experiment. For most experiments, a total of 21−25 injections of a 4 μL injection volume were made at 240 s intervals. In some cases, an initial pre-injection of 2 μL volume was made and the result from this injection was not used for data analysis. The enzyme was prepared for ITC by dialysis overnight against the desired buffer for the particular experiment. The dialysis buffer concentration was either 50 or 100 mM and also contained 10% glycerol and 5 mM 2-mercaptoethanol. The dialysis buffer was used to make up the ligand solution for the injection syringe to match pH and the buffer concentration between the solutions in the stirred cell and the injection syringe. The pH of the ITC experiments was 7.2−7.5. Blank titrations were done in the absence of the enzyme to control for heats of dilution and mixing. The control titrations were subtracted from the experimental titrations prior to data analysis. The data were analyzed by the Origin software provided by MicroCal, Inc. In most cases, the data were fitted to a single-site model (*7*, *8*).

Initial Velocity Studies. Initial velocity data were collected on a Beckman 640 UV/vis spectrophotometer in 1 cm pathlength cuvettes and 1 mL volumes. Assays were done at 25 °C. Typical assays contained 100 mM K^+Hepes at pH 8, 30 mM KCl, and fixed or varied concentrations of uncomplexed Mn^{2+}, uncomplexed NAD, uncomplexed D-malate, or uncomplexed (+)-tartrate, depending upon the experiment; uncomplexed indicates corrections were made for the formation of the chelate complex between the substrates and the divalent metal ion (*9*). The appearance of NADH was followed at 340 nm (ϵ = 6220 M^{-1} cm^{-1}). For initial velocity studies using K^+ as a pseudosubstrate, the enzyme was dialyzed overnight versus 100 mM Tris(HCl) buffer at pH 7.5 containing 10% glycerol and 5 mM 2-mercaptoethanol, and the buffer used in the initial velocity assays was 100 mM Tris(HCl) at pH 8. Initial velocity data were fitted using BASIC versions of the Fortran programs developed by Cleland (*10*). Sequential initial velocity data were fitted using eq 1, and equilibrium-ordered initial velocity data were fitted using eq 2

$$v = \frac{VAB}{K_{ia}K_b + K_aB + K_bA + AB} \quad (1)$$

$$v = \frac{VAB}{K_{ia}K_b + K_bA + AB} \quad (2)$$

where v is the initial velocity, V is the maximum velocity, K_a and K_b are the Michaelis constants for A and B, respectively, K_{ia} is the dissociation constant for A, and A and B are substrate concentrations.

RESULTS

The binding of several substrates and inhibitors to TDH was examined by ITC, which allows, in one experiment, the determination of the association/dissociation constants, enthalpy, and stoichiometry of binding. The $\Delta G°$ of binding may be calculated using the relationship $\Delta G° = -RT \ln K$, where R is the gas constant, T is the temperature, and K is the association constant. The entropy of binding $\Delta S°$ may be calculated from $\Delta G° = \Delta H° - T\Delta S°$.

The ITC data for binding of ligands to TDH are summarized in Table 1. For all but one of the ligands examined, the data were fitted best to a model that specifies one set of sites. However, for NAD, the data fitted best to a model that specifies two interacting sites per dimer for E/K^+ or $E/K^+/Mn^{2+}$ and two independent sites (one per monomer) for $E/K^+/Mg^{2+}$. A binding isotherm and the fitted data for binding of NAD to E/K^+ are shown in Figure 1. The NAD titration was repeated several times with similar results. The binding of NAD to $E/K^+/Mn^{2+}$ gave a higher affinity site with a K_d of about 19 μM and a lower affinity site with a K_d of about 150 μM. In contrast to NAD, the binding isotherm for the reduced dinucleotide substrate, NADH, fitted best to a model with one site per enzyme dimer. An attempt to titrate the $E/K^+/Mn^{2+}$/NADH complex of TDH with NAD gave no evidence for binding of NAD. Evidence for weak binding of NAD to E in the absence of both K^+ and Mn^{2+} was obtained in an ITC titration, but the binding isotherm was not well enough defined to obtain an adequate fit of the data to any model. The only case that exhibited a positive $\Delta H°$ of binding was that of Mn^{2+}; an example of a binding isotherm and fitted data for Mn^{2+} binding to E/K^+ is shown in Figure 2.

The substrate *meso*-tartrate was found to bind to $E/K^+/Mn^{2+}$ with a dissociation constant of about 70 μM and a negative $\Delta H°$. The heat capacity change (ΔC_p) associated with ligand binding may be determined by acquiring the binding isotherm at different temperatures and then fitting the data to $\Delta C_p = (\Delta H°_1 - \Delta H°_2/T_1 - T_2)$. There is a significant temperature dependence for $\Delta H°$ associated with *meso*-tartrate binding giving an estimate of -1.6 ± 0.2 kcal mol^{-1} K^{-1} for ΔC_p. In contrast to *meso*-tartrate, no evidence could be obtained for the binding of D-malate to the $E/K^+/Mn^{2+}$ complex. In addition, no evidence for the binding of

Table 1: Summary of ITC Data for TDH

ligand	T	N^a	K_1 (μM)	K_2 (μM)	ΔH°_1 (kcal/mol)	ΔH°_2 (kcal/mol)	ΔG° (kcal/mol)	ΔS°_1 (kcal mol^{-1} K^{-1})	ΔG°_2 (kcal/mol)	ΔS°_2 (kcal mol^{-1} K^{-1})
Mn (E/K$^+$)[b]	15	1.02[c]	93		+9.59		−5.31	+51.7		
Mn (E/K$^+$)	25	0.94	90		+9.41		−5.52	+50.1		
Mn (E/K$^+$/NAD)	11	0.99	75		+8.15		−5.53	+46.7		
Mn (E/K$^+$/NAD)	20	1.11	64		+11.3		−5.45	+59.0		
NADH (E/K$^+$/Mn^{2+})	16	1.06	31		−16.6		−5.96	−36.8		
NAD (E/K$^+$/Mn^{2+})	16	2.18	19	159	−7.37	−20.0	−6.45	−3.2	−5024	−51.8
NAD (E/K$^+$/Mg^{2+})	16	2	82		−17.1		−5.40	−40.6		
NAD (E/K$^+$)	16	2	54	79	−9.60	−16.0	−5.65	−13.7	−5426	−14.4
meso-tartrate (E/K$^+$)	10	0.96	49		−16.4		−5.58	−38.4		
	17	0.83	71		−27.0		−5.51	−74.2		
	20	0.93	83		−32.7		−5.41	−93.1		
oxalate (E/K$^+$/Mn^{2+}/NAD)	17	0.99	27		−2.69		−6.05	−11.6		
oxalate (E/K$^+$/Mn^{2+}/NADH)	17	0.97	1.2		−3.46		−7.88	−15.2		
oxalate[d] (E/K$^+$/Mn^{2+}/NADH)	17	1.1	3.9		+3.95		−7.38	−11.8		

[a] The stoichiometry (N) refers to binding of ligand per enzyme dimer. [b] The enzyme form titrated is indicated in parentheses. [c] All titration data were fitted to a one-set-of-sites model with the exception of the titrations of E/K$^+$/Mn^{2+} and E/K$^+$ with NAD, which were fitted to a two-interacting-site model. The errors on the fitted parameters listed in the table are all less than 10%. [d] The titration was done in Tris buffer; all other titrations were done in Hepes buffer.

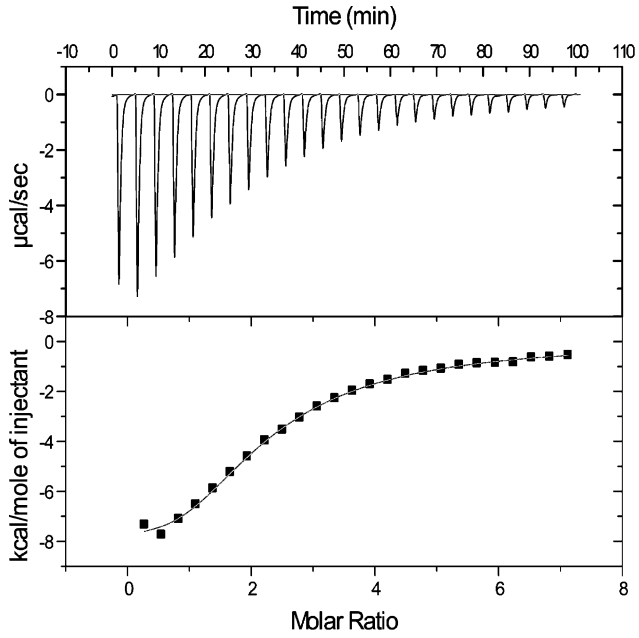

FIGURE 1: Titration of E/K$^+$ with NAD. The cell contained 0.217 mM TDH monomer concentration in 100 mM Hepes at pH 7.5, 4 mM 2-mercaptoethanol, 8% glycerol, and 30 mM added KCl. The syringe contained 10 mM NAD in the same buffer. A total of 25 injections were made at 240 s intervals. (Top panel) Raw ITC data. (Bottom panel) Data after the subtraction of the control titration and peak integration. The solid line is the fit to a model that requires two interacting sites.

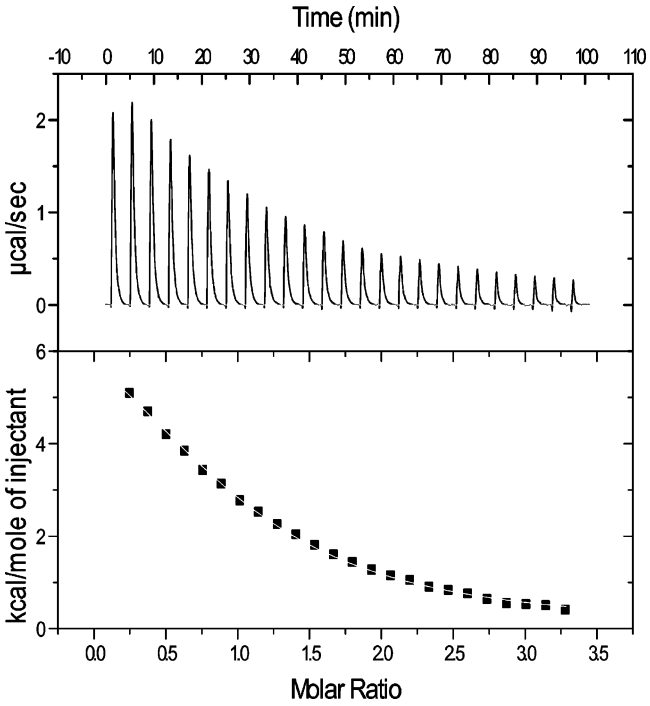

FIGURE 2: Titration of TDH with Mn^{2+}. The cell contained 0.21 mM TDH monomer concentration in 100 mM Hepes at pH 7.2, 4 mM 2-mercaptoethanol, and 8% glycerol. The syringe contained 4 mM $MnSO_4$ in the same buffer. A total of 25 injections were made at 240 s intervals. (Top panel) Raw ITC data. (Bottom panel) Data after the subtraction of the control titration and peak integration. The solid line is the fit to a one-site binding model.

meso-tartrate could be obtained in the presence of Mn^{2+} and the absence of K$^+$.

Oxalate is considered an analogue of the enolpyruvate intermediate formed during the oxidative decarboxylation reaction of D-malate catalyzed by TDH. Oxalate binds to the E/K$^+$/Mn^{2+}/NADH complex with a low K_d of about 1 μM and to the E/K$^+$/Mn^{2+}/NAD complex but with a higher K_d of about 27 μM. The ΔH° of binding for oxalate to the E/K$^+$/Mn^{2+}/NADH complex is dependent upon the buffer used in the experiment. A ΔH° of +3.95 kcal/mol is observed with Tris buffer, while −3.46 kcal/mol is obtained with Hepes buffer; consequently, the values of ΔH° in Table 1 are apparent values. An estimate of the actual value for ΔH° can be determined from a plot of the apparent ΔH° and the ΔH° of ionization of the two buffers (*11*) (see the Discussion). In the absence of a dinucleotide substrate, no evidence for binding of oxalate could be detected to the E/K$^+$/Mn^{2+} complex.

Initial Velocity Studies. The previously reported kinetic mechanism for TDH was proposed to be ordered with the order of addition as Mn^{2+}, NAD, and D-malate (*1*). However, some of the complexes identified by ITC experiments are not predicted by the ordered mechanism. In addition, the

Table 2: Steady-State Kinetic Parameters for TDH[a]

variable substrate	fixed variable substrate	fixed substrate	K_m (mM)	K_{ia} (mM)	intersection point
D-malate	NAD	Mn (2 mM) K^+ (>30 mM)	0.090 (0.018) D-malate 0.143 (0.039) NAD		left of the ordinate
Mn^{2+}	D-malate	NAD (1.5 mM) K^+ (>30 mM)	0.092 (0.015) D-malate	0.11 (0.018) Mn^{2+}	on the ordinate
K^+	D-malate	NAD (1.5 mM) Mn^{2+} (0.2 mM)	0.43 (0.08) D-malate	4.2 (0.8) K^+	on the ordinate
K^+	NAD	D-malate (2 mM) Mn^{2+} (0.2 mM)	0.134 (0.026) NAD	32 (7) K^+	on the ordinate
K^+	NAD	D-malate (0.2 mM) Mn^{2+} (0.2 mM)	0.148 (0.022) NAD	29 (5) K^+	on the ordinate
Mn^{2+}	NAD	(+)-tartrate (4 mM) K^+ (>30 mM)	0.38 (0.09) NAD 0.014 (0.005) Mn^{2+}		left of the ordinate
Mn^{2+}	NAD	D-malate (0.1 mM) K^+ (>30 mM)	0.18 (0.03) NAD 0.055 (0.009) Mn^{2+}		left of the ordinate

[a] Values in parentheses are standard errors.

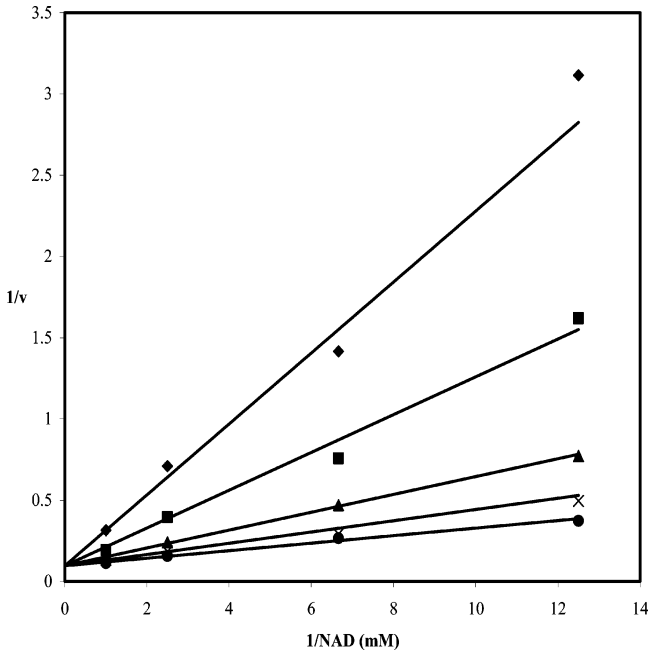

FIGURE 3: Initial velocity pattern for NAD versus K^+. The buffer was 100 mM Tris (HCl) at pH 7.5, and fixed substrate concentrations were 0.2 mM Mn^{2+} and 2 mM D-malate. The K^+ concentrations were (◆) 2 mM, (■) 4 mM, (▲) 10 mM, (×) 20 mM, and (●) 45 mM. The initial rate (v) is in micromolar per minute.

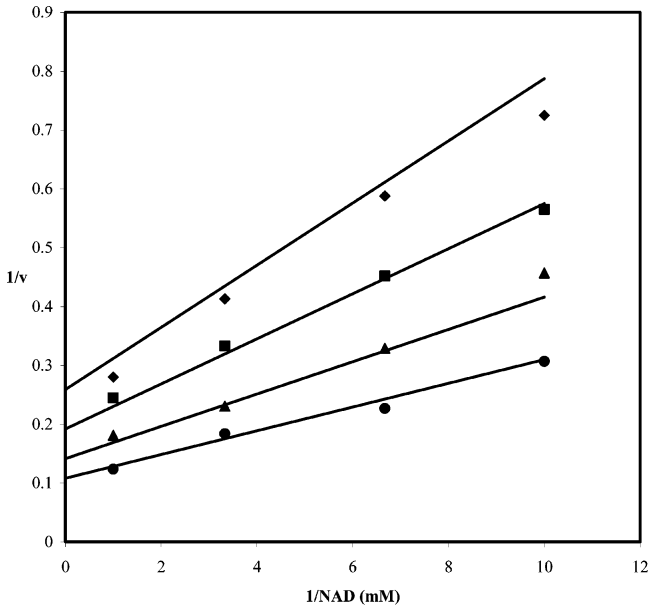

FIGURE 4: Initial velocity pattern for NAD versus Mn^{2+}. The buffer was 100 mM Hepes at pH 7.5, and the fixed substrate concentrations were 0.1 mM D-malate and >30 mM K^+. The Mn^{2+} concentrations were (◆) 0.03 mM, (■) 0.05 mM, (▲) 0.1 mM, and (●) 0.3 mM. The initial rate (v) is in micromolar per minute.

reported kinetic mechanism did not consider the order of binding of the monovalent ion in the mechanism. These observations prompted a re-examination of the kinetic mechanism by initial velocity studies. Initial velocity patterns are summarized in Table 2. The K^+ versus NAD pattern appears to intersect on the ordinate as shown in Figure 3. The D-malate versus Mn^{2+} pattern also intersects on the ordinate, indicating an equilibrium-ordered addition of Mn^{2+} prior to malate, while the NAD versus Mn^{2+} pattern intersects to the left of the ordinate as shown in Figure 4, which differs from earlier work. The K^+ versus D-malate pattern also intersects on the ordinate, indicating an equilibrium-ordered addition, while the remaining patterns intersect to the left of the ordinate.

DISCUSSION

Half-of-the-Sites Reactivity. One of the most interesting aspects to come out of the ITC binding studies is that, with the exception of NAD, all of the substrate and inhibitors tested bound to the enzyme dimer with a stoichiometry of 1. There is currently no crystal structure available for TDH; however, the presumption is that the homodimeric enzyme contains two active sites and results with NAD indicate this. However, even in cases where NAD is present in the titration, other ligands such as oxalate or Mn^{2+} bind with a stoichiometry of 1 per dimer. The results suggest the possibility of a half-of-the-sites or reciprocating-sites (flip-flop) mechanism for TDH. The enzyme may have a natural asymmetry to its structure that allows only one active site to bind most ligands. It is worth noting that, with NAD, the higher affinity site has a K_d of about 20 μM, while the lower affinity site has a K_d of about 150 μM. The K_m for NAD is about 150 μM and suggests that the lower affinity site is the functional active site, assuming that the K_m is similar to the K_d. It is also interesting that NADH binds to enzyme with a stoichiometry of 1 per enzyme dimer. In a titration of the enzyme in the presence of saturating NADH, in which one active site is presumably occupied by NADH, a titration with NAD did not lead to evidence for the binding of NAD to the second

active site. Apparently, once NADH is bound to one active site, the other site is inaccessible to NAD. It is not clear from the current data whether, once an enzyme turnover occurs at the functional active site, an enzyme conformational change ensues that allows for the formally inactive site to become the functional one and visa versa.

meso-Tartrate Binding. The TDH kinetic mechanism appears to require all cofactors (Mn^{2+} and K^+) and NAD to bind before D-malate or (+)-tartrate (see below). The substrate *meso*-tartrate is an exception in that it can bind in the absence of NAD to the E/Mn^{2+}/K^+ complex. TDH has about 38% identity to isopropylmalate dehydrogenase, and it has been proposed that isopropylmalate dehydrogenase (IPMDH) is the evolutionary progenitor of TDH (*2*). IPMDH has a hydrophobic pocket that accommodates the isopropyl group of the isopropylmalate substrate (*12*−*15*), and TDH presumably retains this hydrophobic pocket in some manner. The binding of *meso*-tartrate is associated with a large negative ΔC_p, normally attributed to the formation of hydrophobic interactions upon binding the substrate (*16*). It does not seem likely that the relatively small and negatively charged *meso*-tartrate could lead to such a large negative ΔC_p even if it does interact in some way with a hydrophobic pocket within the enzyme binding site. The binding energy for *meso*-tartate is likely derived from the charged carboxyl groups and the polar hydroxyl groups interacting with the bound Mn^{2+} and K^+ ions; both are required for *meso*-tartrate binding. The large negative ΔC_p associated with *meso*-tartrate binding likely results from an induced protein conformational change leading to desolvation and formation of hydrophobic interactions within the protein. It has been proposed previously that there may be different modes of binding of the dicarboxylic acid substrates of TDH (*12*). The observed binding of *meso*-tartrate to the E/Mn^{2+}/K^+ complex, while D-malate cannot bind to this complex, is consistent with different binding modes for the two substrates. The different manner in which *meso*-tartrate and D-malate bind to the enzyme may be what results in the significant protein conformational change suggested by the ΔC_p data.

Divalent Metal Ion Binding. The divalent metal ion Mn^{2+} binds to both E/K^+ and E/K^+/NAD complexes with about equal affinity and with a stoichiometry of binding of 1 per dimer. The divalent metal ion is the only ligand tested that exhibits entropically driven binding (Table 1). For a ligand such as *meso*-tartrate, negative contributions to $\Delta S°$ would generally come from losses in rotational, vibrational, and translational degrees of freedom upon the formation of the complex. These negative contributions to $\Delta S°$ come from losses in conformational flexibility in the ligand and/or protein upon the formation of the complex. In solution, Mn^{2+} would have only translational degrees of freedom to lose. Upon binding to the enzyme, the translational motion of Mn^{2+} would be lost but the translational motion of the enzyme would be retained in the complex. The loss of one translational degree of freedom and whatever conformational flexibility of the protein is lost upon binding the divalent metal ion are not enough to overcome the positive contributions to $\Delta S°$. Favorable contributions to $\Delta S°$ usually involve the release of ordered water molecules into the bulk solvent. On the basis of homology to IPMDH, the divalent metal ion likely coordinates to aspartate residues D225, D250, and D254. The binding of Mn^{2+} likely displaces waters that are coordinated to the metal ion as it forms coordination bonds with the aspartate residues.

Oxalate Binding. Oxalate is considered an analogue of the enolpyruvate intermediate that would be formed in the TDH-catalyzed oxidative decarboxylation of D-malate. Oxalate was shown to be a slow-binding inhibitor of TDH under initial velocity turnover conditions. In addition, the slow addition of oxalate to an E/Mn^{2+}/NADH complex could be followed by changes in intrinsic enzyme fluorescence. The maximum rate of first-order decay of the enzyme fluorescence upon addition of oxalate was about 0.09 s^{-1} (*4*). Examination of oxalate binding by ITC gave a stoichiometry of binding of 1 per dimer to either the E/K^+/Mn^{2+}/NAD or E/K^+/Mn^{2+}/NADH complex. The K_d for binding of oxalate to the NAD complex is about 27 μM and about 1 μM to the NADH complex. The K_d value for binding to the NADH complex is similar to the previously reported value, but the previously reported value for the NAD complex was about 80 μM. In any case, oxalate binds to the NADH complex about 10-fold better than when NAD is bound. During enzyme turnover, the enolpyruvate intermediate would be formed with NADH bound; it is reasonable that an analogue of enolpyruvate would bind with greater affinity to the NADH complex. Oxalate did not bind in the absence of a dinucleotide substrate and indicates the requirement for either NAD or NADH for oxalate binding.

The apparent enthalpy of binding of oxalate to E/K^+/Mn^{2+}/NADH is dependent upon the buffer used in the titration. The heat of ionization of Tris buffer is +11.3 kcal/mol at 25 °C (*17*), and the heat of ionization of Hepes buffer has been reported as +3.92 (*17*) and +4.99 kcal/mol (*18*). If proton(s) are taken up by the protein during the binding process, the $\Delta H°$ will reflect both the $\Delta H°$ associated with the binding of oxalate and the $\Delta H°$ associated with the loss of a proton by the buffer. Using an average value of +4.46 kcal/mol for $\Delta H°_{ion}$ of Hepes, the difference in the $\Delta H°_{ion}$ for Tris and Hepes is 6.84 kcal/mol. The difference in $\Delta H°$ for oxalate binding in Tris and Hepes buffer is 7.41 kcal/mol and suggests that oxalate binding to the enzyme requires a proton. The true ΔH for oxalate binding can thus be calculated by plotting apparent $\Delta H°$ versus $\Delta H°_{ion}$ of the buffer and, for oxalate binding to the NADH complex, gives a value for $\Delta H°$ of about 8.7 kcal/mol. The entropy associated with the binding of oxalate to the NADH complex can be calculated as −2.8 cal mol^{-1} K^{-1} in Hepes and −4.5 cal mol^{-1} K^{-1} in Tris buffer. The uptake of a proton on oxalate binding is reasonable because during turnover the general base would accept a proton from the 2-hydroxyl of malate during hydride transfer to form NADH. During the subsequent decarboxylation step, a proton would be shuttled from the general base back to form enolpyruvate. Thus, the NADH complex would favor the protonated general base.

The small unfavorable entropy term associated with oxalate binding may come from losses in rotational, vibrational, and translational freedom of oxalate. Oxalate is reported to be a slow-binding inhibitor of TDH, and it was proposed that following the formation of the initial E/oxalate complex a conformational change occurs to form the tight E/oxalate complex. Although the ITC titration results with oxalate did not reveal evidence for the slow-binding behavior of oxalate, a protein conformational change associated with oxalate binding is probable given the reported slow-binding

Scheme 1: Kinetic Mechanism for TDH[a]

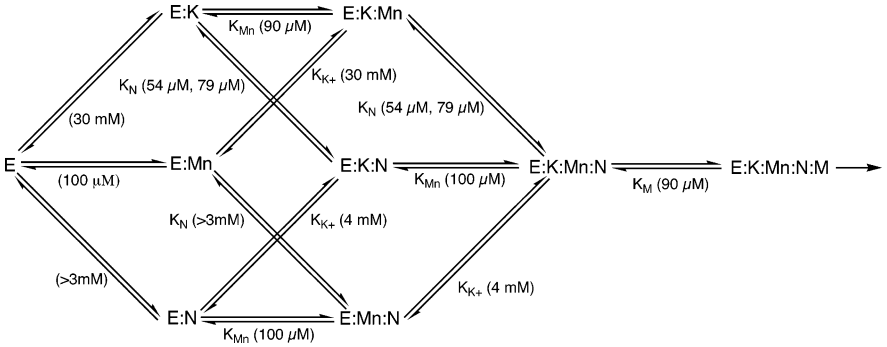

[a] The scheme shows dissociation and Michaelis constants, where known, associated with enzyme−substrate complexes. Estimated values of dissociation constants are shown in parentheses. The Michaelis constant is given for D-malate. In the scheme, K = K^+, Mn = Mn^{2+}, N = NAD, and M = D-malate.

inhibitory behavior of oxalate. The entropically unfavorable protein closure likely associated with oxalate binding may be compensated by other effects, such as desolvation of oxalate, that lead to the relatively small unfavorable entropy term for oxalate binding.

Kinetic Mechanism. The kinetic mechanism for TDH was re-examined in light of the ITC results. The previously proposed ordered mechanism of Mn^{2+}, followed by NAD and then D-malate or (+)-tartrate would predict that NAD cannot bind in the absence of Mn^{2+}. The ITC results clearly indicate that in the absence of Mn^{2+} the addition of NAD to E/K^+ occurs with a binding constant similar to the K_m for NAD. Initial velocity patterns were obtained to investigate the kinetic mechanism. When the initial rate is measured as a function of D-malate at different fixed levels of Mn^{2+}, the pattern intersects on the ordinate, indicative of equilibrium-ordered addition of the metal ion prior to D-malate. The ITC results indicate that D-malate does not bind to the E/K^+/Mn^{2+} complex unless NAD is bound, and thus, D-malate binds to the E/K^+/Mn^{2+}/NAD complex. However, ITC results suggest NAD can bind to both the E/K^+ and E/K^+/Mn^{2+} complexes, so that the divalent metal ion is not required for NAD binding. These results are in contrast to previously reported results (*1*) that suggested equilibrium-ordered addition of Mn^{2+} prior to NAD. An ITC titration of E by NAD in the absence of both Mn^{2+} and K^+ suggests weak binding of NAD to free E. Initial velocity data obtained varying K^+ and NAD give an estimate of about 30 mM for K_{K^+}, and it is reduced to about 4 mM at saturating NAD. The 7-fold difference in the binding constant for K^+ binding to the free enzyme (30 mM) and E/NAD (4 mM) likely leads to the apparent equilibrium-ordered pattern for K^+ versus NAD; i.e., the addition of the two is equilibrium-random with synergism. Fluorescence titrations of TDH with K^+ at high NAD concentrations (data not shown) also lead to an estimate of 3−4 mM for K_{K^+}.

In summary, the kinetic mechanism for TDH appears to be random with respect to the binding of NAD, K^+, and Mn^{2+}, but there is a requirement that all three be bound to the enzyme before D-malate can bind. The binding of NAD and K^+ is synergistic. The kinetic mechanism associated with binding of substrates to TDH is shown in Scheme 1. In most cases, the measured dissociation constant is given for the binding of each substrate to each complex in Scheme 1. Although the dissociation constant for Mn^{2+} binding to E and E/NAD was not directly determined in the current work, the values are estimated at about 100 μM because the Mn^{2+} dissociation constant is about 100 μM to both E/K^+ and E/K^+/NAD. At a low K^+ concentration, a K_m value for NAD of about 3 mM was measured from initial velocity data varying NAD. The K_d for NAD in the absence of K^+ is likely at least 3 mM. The kinetic mechanism with *meso*-tartrate as a substrate is different because it can bind to E/K^+/Mn^{2+} with a dissociation constant similar to its reported K_m value. Although *meso*-tartrate does not require NAD to be on the enzyme, this substrate requires prior binding of K^+ and likely the divalent metal ion. Thus, with *meso*-tartrate, there is random addition of *meso*-tartrate and NAD, opposed to the ordered addition of NAD prior to D-malate.

The role of the monovalent cation in the reaction is rather interesting in that it appears to be required for D-malate binding and enhances NAD binding. Data suggest the monovalent cation may play a direct role in D-malate binding. However, with just one exception, all of the amino acid residues that are proposed to line the isopropylmalate site in IPMDH are retained in TDH (*2*, *13*−*15*) and none of these residues seems to be a likely candidate for binding a monovalent cation. Using the numbering for TDH, there are three aspartate residues (D225, D250, and D254) that appear to be the ligands to the divalent metal ion. There are arginine residues (R98 and R108) that likely are involved in substrate binding and two residues proposed to be catalytic residues (K192 and Y141). In the *Thermus thermophilus* IPMDH, there are two leucine residues retained in TDH that line the hydrophobic pocket of the isopropylmalate site and E87, for which the methylene groups contribute to the hydrophobic pocket, and the γ carboxylate is proposed to interact with the nicotinamide of NAD; in TDH, E87 is replaced by W91. Exactly where the monovalent metal ion may bind to the enzyme and yet have such a profound effect on the binding of both D-malate and NAD is still an open question, and additional studies will be required to resolve this question.

REFERENCES

1. Tipton, P. A., and Peisach, J. (1990) Characterization of the Multiple Catalytic Activities of Tartrate Dehydrogenase, *Biochemistry 29*, 1749−1756.
2. Tipton, P. A., and Beecher, B. S., (1994) Tartrate Dehydrogenase, A New Member of the Family of Metal-Dependent Decarboxylating *R*-Hydroxyacid Dehydrogenases, *Arch. Biochem. Biophys. 313*, 15−21.
3. Karsten, W. E., Tipton, P. A., and Cook P. F. (2002) Tartrate Dehydrogenase Catalyzes the Stepwise Oxidative Decarboxylation

of D-Malate with both NAD and Thio-NAD, *Biochemistry 41*, 12193−12199.
4. Beecher, B. S., Koder, R. L., and Tipton, P. A. (1994) Tartrate Dehydrogenase−Oxalate Complexes: Formation of a Stable Analog of a Reaction Intermediate Complex, *Arch. Biochem. Biophys. 315*, 255−261.
5. Bradford, M. (1976) A Rapid and Sensitive Method for the Quantitation of Microgram Quantities of Protein Utilizing the Principle of Protein−Dye Binding, *Anal. Biochem. 72*, 248−254.
6. Tipton. P. A. (1996) Transient-State Kinetic Analysis of the Oxidative Decarboxylation of D-Malate Catalyzed by Tartrate Dehydrogenase, *Biochemistry 35*, 3108−3114.
7. Wiseman, T., Williston, S., Brandts, J. F., and Lin, L. N. (1989) Rapid Measurement of Binding Constants and Heats of Binding Using a New Titrating Calorimeter, *Anal. Biochem. 179*, 131−137.
8. Indyk, L., and Fisher, H. F. (1998) Theoretical Aspects of Isothermal Titration Calorimetry, *Methods Enzymol. 295*, 350−364.
9. Park, S.-H, Kiick, D. M., Harris, B. G., and Cook, P. F. (1984) Kinetic Mechanism in the Direction of Oxidative Decarboxylation for NAD−Malic Enzyme from *Ascaris suum*, *Biochemistry 23*, 5446−5453.
10. Cleland, W. W. (1979) Statistical Analysis of Enzyme Kinetic Data, *Methods Enzymol. 63*, 103−108.
11. Parker, M. H., Lunney, E. A., Ortwine, D. F., Pavlovsky, A. G., Humblet, C., and Brouillette, C. G. (1999) Analysis of the Binding of Hydroxamic Acid and Carboxylic Acid Inhibitors to the Stromelysin-1 (Matrix Metalloproteinase-3) Catalytic Domain by Isothermal Titration Calorimetry, *Biochemistry 38*, 13592−13601.
12. Serfozo, P., and Tipton, P. A. (1995) Substrate Determinants of the Course of Tartrate Dehydrogenase-Catalyzed Reactions, *Biochemistry 34*, 7517−7524.
13. Kadono, S., Sakurai, M., Moriyama, H., Mamoru, S., Hayashi, Y., Oshima, T., and Tanaka, N. (1995) Ligand-Induced Changes in the Conformation of 3-Isopropylmalate Dehydrogenase from *Thermus thermophilus*, *J. Biochem. 118*, 745−752.
14. Zhang, T., and Koshland, D. E. (1995) Modeling Substrate Binding in *Thermus thermophilus* Isopropylmalate Dehydrogenase, *Protein Sci. 4*, 84−92.
15. Dean, A. M., and Dvorak, L. (1995) The Role of Glutamate 87 in the Kinetic Mechanism of *Thermus thermophilus* Isopropylmalate Dehydrogenase, *Protein Sci. 4*, 2156−2167.
16. Spolar, R. S., Livingstone, J. R., and Record, M. T., Jr. (1992) Use of Liquid Hydrocarbon and Amide Transfer Data To Estimate Contribution to Thermodynamic Functions of Protein Folding from the Removal of Nonpolar and Polar Surface from Water, *Biochemistry 31*, 3947−3955.
17. Grime, J. K. (1985) in *Analytical Solution Calorimetry* (Grime, J. K., Ed.) pp 299−390, Wiley and Sons, New York.
18. Fukada, H., and Takahashi, K. (1998) Enthalpy and Heat Capacity Changes for the Proton Dissociation of Various Buffer Components in 0.1 M Potassium Chloride, *Proteins 33*, 159−166.

BI0607251